EPJ Web of Conferences **274**, 05001 (2022) https://doi.org/10.1051/epjconf/202227405001
XVth Quark Confinement and the Hadron Spectrum

Rapidity-dependent charge-dependent flow, global polarisation and chiral magnetic effect in heavy ion collisions

Shi Qiu[1,2,*]

[1]Nikhef
[2]Utrecht University

Abstract. An extremely strong magnetic field (as strong as 10^{15} T) is created in the off-central heavy-ion collisions by the spectator protons which "miss" the collisions, flying past each other rather than colliding. The magnetic field is interesting to be studied as it is expected to leave distinct imprints in the distribution of final state charged particles. In addition, novel QCD phenomena are anticipated to emerge with the presence of a strong magnetic field and the formation of charge-parity violating domains inside the medium produced in heavy-ion collisions. The aim of this article is to review two methods utilised by the experimental searches to probe the early magnetic field: the directed flow of charged hadrons (and heavy-flavour hadrons D^0 and $\bar{D}^0$) and the global polarisation of Λ and $\bar{\Lambda}$ hyperons. Furthermore, this article is also dedicated to review the searches for one of the novel QCD phenomena, the chiral magnetic effect, at the LHC and RHIC.

1 Introduction

Quantum Chromo-dynamic (QCD) calculations on the lattice indicates the existence of a deconfined state of quarks and gluons, known as the quark-gluon plasma (QGP), at high temperature and energy density. In the Large Hadron Collider (LHC) and the Relativistic Heavy Ion Collider (RHIC), the collisions of two heavy-ion particles at ultrarelativistic energy create a lab to study the properties of QGP. In the earliest moments after noncentral heavy-ion collisions, an extremely strong magnetic field, of the order of $eB \sim 10^{15}$ T, is created by the spectator protons which “miss”, flying past each other rather than colliding [1–3].

It is of great experimental interest to measure the magnitude of the early magnetic field directly. Albeit decreasing fast in time, this magnetic field is expected to influence the charge dynamics with complicated interplay of the Faraday effect, and Lorentz and Coulomb forces in the QGP, which leads to potential characteristic imprints on experimental observables [4–6]. In general, four types of currents will be created: Farady current, Lorentz current, Coulomb current and plasma current. The first three effects mainly result in a net rapidity-odd charge-odd directed flow (Δv_1) and the last effect results in a non-trivial radial and elliptic flow. In addition, it was also predicted in [6] that a charge-odd triangular flow Δv_3 that is odd in rapidity arises from a a similar physical origin as Δv_1 and the strong Coulomb forces from the electric field created by net charge density of the plasma leads to a rapidity-even

*e-mail: s.qiu@nikhef.nl

charge-odd elliptic flow Δv_2. Section 2 will be dedicated to the measurement of the rapidity-dependent charge-dependent flow at the LHC and similar measurements at lower energies and a different collision system from the STAR collaboration at RHIC.

The early magnetic field can be probed from a completely different perspective: the hyperon–anti-hyperon global spin polarization asymmetry, which is a measurement of the degree of alignment of hyperons' or anti-hyperons' spin with a given direction, in this case the spectator plane which is strongly correlated to the direction of the magnetic field [7]. The Λ and $\bar{\Lambda}$ are experimentally favourable because the protons emitted from its dominant decay channel, ($\Lambda(\bar{\Lambda}) \rightarrow p(\bar{p}) + \pi^-(\pi^+)$), align preferentially to the direction of the $\Lambda(\bar{\Lambda})$ spin. The main mechanism for the global polarisation effect comes from the large fluid vorticity, ω, generated from two colliding heavy-ions moving in opposite directions with velocity close to the speed of light. Orbital angular momentum is transferred to particle spin equally for particles and antiparticles. The magnetic field as a secondary effect, pointing in the same direction as the average vorticity, align particles' and antiparticles' spin oppositely due to the opposite sign of magnetic moment. The relationship can be written in following approximate forms: $P_\Lambda \approx 0.5\omega/T + |\mu_\Lambda|B/T$ and $P_\Lambda \approx 0.5\omega/T - |\mu_\Lambda|B/T$, where μ_Λ is the the Λ magnetic moment and T is the system temperature. Therefore, taking the difference between the global polarisation of Λ and $\bar{\Lambda}$ largely cancels out the effect of fluid vorticity and provides an alternative way to probe the magnetic field at freeze-out. In section 3, the measured global polarisation of Λ hyperon–anti-hyperon in Pb-Pb collisions at $\sqrt{s_{NN}}$ = 2.76 and 5.02 TeV with the ALICE collaboration and in Au-Au collisions at various lower energies from the STAR collaboration are presented and discussed.

Heavy-ion collisions provide a unique environment to study novel QCD phenomena with the presence of a strong magnetic field, in particular the local parity and charge conjugation parity symmetry violation in the strong interaction. The QGP produced at high temperatures, the situation for heavy-ion collisions, permits the transitions between two vacuum states with different topological quantum numbers not only through instantons (tunneling through the potential barrier) but also through sphalerons (jumping over the potential barrier) (see e.g. [8–10]), which causes the creation of local domains of non-conserving chirality, e.g. more left-handed quarks than right-handed quarks. Several interesting effects rises due to the interplay between these magnetic fields and quantum anomalies, such as the chiral magnetic effect (CME) and the chiral magnetic wave (CMW). This article focuses on the former one. As proposed by [11–14], the chiral magnetic effect happens when a strong magnetic field is present around the domains of chirality imbalance. The magnetic field aligns the quarks' spin preferably along the magnetic field direction and the momentum direction of quarks with specific chirality align accordingly to their spin orientation. This leads to a global electric charge separation with respect to the reaction plane defined by the impact parameter and the beam axis with the strength of the charge separation proportional to the amount of chirality imbalance and the strength of the magnetic field. The discovery of the chiral magnetic effect would directly provide answer to one of the biggest puzzles in the Standard model—the strong CP (charge conjugation parity) problem: why CP-symmetry is preserved in the strong interactions. Section 4 will mainly focus on the search for CME in Pb-Pb collisions at $\sqrt{s_{NN}}$ = 2.76 and 5.02 TeV and Xe-Xe collisions at $\sqrt{s_{NN}}$ = 5.44 TeV from the LHC. The searches in Au-Au collisions and isobar collisions (Ru-Ru and Zr-Zr) both at $\sqrt{s_{NN}}$ = 200 GeV from RHIC will also be discussed.

2 Probe the early magnetic field with rapidity-dependent charge-dependent flow

The rapidity-dependent charge-dependent directed flow of positively, $v_1(h^+)$, and negatively charged hadrons, $v_1(h^-)$, with $p_T > 0.2$ GeV/c for the $5-40\%$ centrality interval relative to the spectator plane was reported by the ALICE collaborations for Pb-Pb collisions at $\sqrt{s_{NN}} = 5.02$ TeV. The Zero Degree Calorimeter (ZDC) measuring spectator neutrons is used to reconstruct the direction of the spectator plane. The $v_1(h^+)$ and $v_1(h^-)$ are plotted with respect to pseudorapidity in the upper right of Fig. 1 to explore the rapidity-odd and charge-odd characteristics [15]. In addition, the same measurement for D^0 ($c\bar{u}$) and $\bar{D}^0$ ($\bar{c}u$) mesons with $3 < p_T < 6$ GeV/c in a centrality range of $10-40\%$ was performed, which has the advantage that charm quarks, due to its heavier mass, are produced mainly through hard binary collisions when the magnetic field is maximal. As a consequence, charm quarks are more strongly affected by the early magnetic field than light quarks, leading to a more prominent charge-odd behaviour (a larger slope in $\Delta v_1(D) = v_1(D^0) - v_1(\bar{D}^0)$), as shown in upper right panel of Fig. 1. The rapidity slope $d\Delta v_1/d\eta$ of charged hadrons and D mesons are plotted in the lower left and right panel of Fig. 1, respectively. The linear function fit yields a gradient of $[1.68 \pm 0.49\,(\text{stat.}) \pm 0.41\,(\text{syst.})] \times 10^{-4}$ for charged hadrons and a three orders of magnitude larger gradient of $[4.9 \pm 1.7\,(\text{stat.}) \pm 0.6\,(\text{syst.})] \times 10^{-1}$ for D mesons, with a significance of 2.6σ and 2.7σ for being positive, respectively.

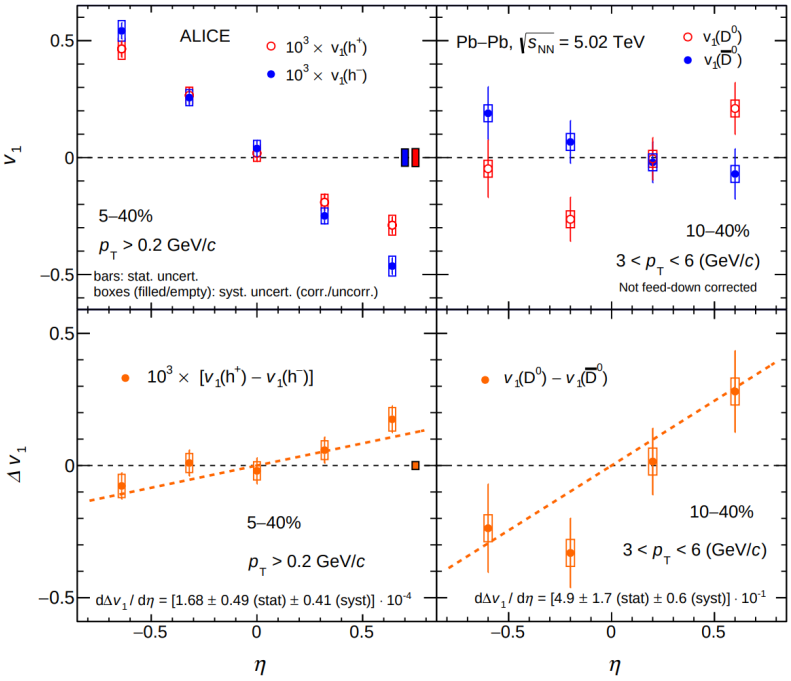

Figure 1: Results from ALICE is chosen to be shown here. Upper left: v_1 of positively (red) and negatively (blue) charged hadrons for the 5–40% centrality interval; upper right: v_1 of D^0 (red) and $\bar{D}^0$ (blue) for the 10–40% centrality interval; lower left and right: $\Delta v_1(h) = v_1(h^+) - v_1(h^-)$ and $\Delta v_1(D) = v_1(D^0) - v_1(\bar{D}^0)$, respectively. Dashed lines represent fits with a linear function [15].

Similar measurements have been performed by the STAR collaborations at RHIC in Au-Au collisions at various low energies (eight in total) ranging from 7.7 GeV up to the top RHIC energies of $\sqrt{s_{NN}}$ = 200 GeV [16, 17]. The energy dependence of the slope of v_1 of pions (π^+ and π^-) and (anti-)protons relative to rapidity is detailed discussed in [4, 16]. Generally, the results of pions and protons from STAR collaboration suggests that the ALICE measurement for unidentified charged hadrons, mainly consist of pions, kaons and protons, can have significantly different contributions from various light-flavour hadrons due to corresponding different physical underlying mechanisms including the early-time magnetic field dynamics, Coulomb interaction with the charged spectators, and baryon transport to midrapidity via baryon stopping, which requires to be understood better [4]. The extracted Δv_1 slope, $d\Delta v_1/d\eta$, for pions and protons was found to be negative and positive, respectively, which again requires to be further studied and more precise and differential measurements at the LHC in Run 3. For heavy-flavour hadrons, the Δv_1 of D mesons measured at midrapidity ($|\eta| < 0.8$) in the 10–80% centrality interval in Au–Au collisions at $\sqrt{s_{NN}}$ = 200 GeV gives a negative slope. The observation of opposite and large slope at the LHC might indicate a stronger effect of the magnetic field (Lorentz force) in comparing to the induced electric field (Coulomb force) and the initial tilt of the source in the reaction plane [18]. Overall, these results provide the experimental hint of the existence of the early electromagnetic fields in the heavy-ion collisions, while high precision and differential measurements are required to draw strong conclusions on the charge transport both for the light- and the heavy-flavor particles. The directed flow of charm quark demonstrates a higher sensitivity to the early magnetic field than light-flavour hadrons.

Moreover, the CMS collaboration at the LHC measured the charge-dependent elliptic flow of D_0 and $\bar{D}_0$ mesons with $2 < p_T < 8$ GeV/c, relative to rapidity for the 20-70% centrality interval in Pb-Pb collisions at $\sqrt{s_{NN}}$ = 5.02 TeV [19]. The splitting of v_2 for D_0 and $\bar{D}_0$, averaged over the full rapidity range, yields $\Delta v_2 = 0.001 \pm 0.001(\text{stat.}) \pm 0.003(\text{syst.})$, which shows no significant deviation from zero within experimental uncertainties. As pointed out in [4], the predicted value of Δv_2 for charged pions in [6] is negative and around the order of magnitude of 10^{-3} at LHC energies. Despite of no significant experimental results, the experimental results might hint a sign opposite to the model.

3 Polarisation of Λ and $\bar{\Lambda}$ hyperons

The global polarisation of Λ and $\bar{\Lambda}$ are reported by both ALICE and STAR collboration. ALICE collboration studied such polarisation at mid-rapidity in mid-central Pb-Pb collisions at $\sqrt{s_{NN}}$ = 2.76 and 5.02 TeV [20]. The magnitudes of the average global polarisation at LHC energies are consistent with expection based on the decreasing trend with the increase of collision energies traced out from the same measurements by the STAR collaboration at RHIC in Au-Au collisions at various lower energies ranging from 7.7 GeV up to $\sqrt{s_{NN}}$ = 200 GeV [21, 22]. No significant splitting between the polarisation ofΛ and $\bar{\Lambda}$ was found at LHC energies, but an upper limit of the magnitude of the magnetic field $eB/m_\pi^2 = 0.017$ (equivalent to 5.7×10^{12} T and 0.044 (or 14.4×10^{12} T) at a 95% confidence level was determined for Pb-Pb collisions at $\sqrt{s_{NN}}$ = 2.76 and 5.02 TeV, respectively. The same upper limits have been determined by the STAR collaboratoin at RHIC in Au-Au collisions at centre-of-mass energies varying from $\sqrt{s_{NN}}$ = 7.7 GeV to 200 GeV. Fig. 2 shows the collision energy dependence of the upper limits of the magnetic field at freeze-out based on the splitting of Λ and $\bar{\Lambda}$ polarisation measured at the LHC and RHIC.

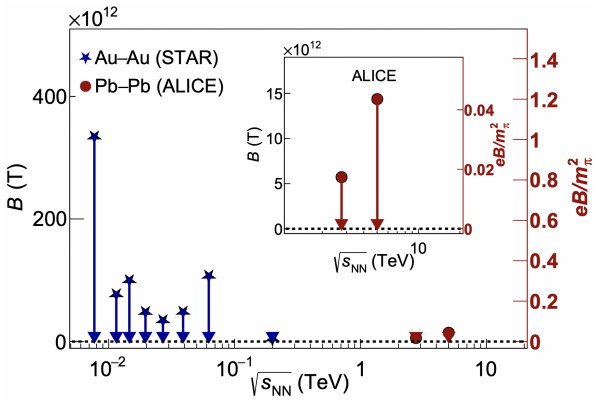

Figure 2: The upper limit of the magnetic field at freeze-out relative to collision energies determined from the global Λ and $\bar{\Lambda}$ hyperon polarisation measured at the LHC and RHIC [20, 21]. This figure is adopted from [23].

4 Experimental searches of chiral magnetic effect

At early time, Voloshin proposed that a way to probe the leading order P-odd coefficient in CME is by measuring charge-dependent azimuthal correlations, relative to the reaction plane, $\Psi_{\rm RP}$ [24]. This charge-dependent azimuthal correlator, known as $\gamma_{1,1}$, is defined as $\gamma_{1,1} = \langle \cos(\varphi_\alpha + \varphi_\beta - 2\Psi_{\rm RP})\rangle$, where the angular brackets indicate an average over all events, and φ represents the azimuthal angle of a track, while α and β indicate either same or opposite charges combinations. The final observable for CME is constructed by taking the difference of opposite- $\gamma_{1,1}$(OS) and same-sign pairs $\gamma_{1,1}$(SS), denoted as $\Delta\gamma$.

Since then, experimental searches have been firstly performed at the STAR Collaboration in Au–Au collisions [25, 26], in which the results were aligned with initial expectations for a charge separation with respect to the reaction plane due to the CME. Soon after the operation of the LHC, the ALICE collaboration reported the measurements of the same correlations for Pb–Pb collisions at $\sqrt{s_{NN}} = 2.76$ TeV [27] and showed a quantitatively similar effect. This is followed by more measurements in Pb-Pb collisions at $\sqrt{s_{NN}} = 5.02$ TeV by both ALICE and CMS collaboration [28, 29]. Recently, the measurements in Xe-Xe collisions were also reported in [30, 31]. However, the observation of quantitative agreement between the same charge-dependent correlation in the LHC and RHIC [25, 26], despite of different collision energies and collision systems leading to different multiplicity densities and magnetic fields, hints that these correlations are heavily contaminated by background effects. The sources of contamination were identified to be mainly from local charge conservation coupled to the anisotropic expansion of the system in noncentral collisions [32, 33].

Several new methods were developed to disentangle the signal and the background in the charge dependent correlators. The ALICE and CMS collaboration presented the upper limit of 26–33% [34] and 7% [35], respectively, at 95% confidence level for the CME contribution using an event shape engineering (ESE) technique proposed in [36]. The main idea of ESE is that at each centrality interval (events with similar impact parameters), the initial geometry of each collision (i.e., the position of participating nucleons) exhibits strong fluctuations, which allows one to select events with different initial system shapes. The dominant component of the background, the elliptic flow coefficient v_2, which is correlated to the initial system shape, can be minimised accordingly. The STAR collaboration combined ESE with cuts on

pair invariant mass to also reduce strong resonance background contributions, concluding an upper limit of 15% at 95% confidence level in Au-Au collisions at $\sqrt{s_{NN}}$ = 200 GeV [37].

The higher harmonic method is another approach attempted by ALICE collaboration. This method constrains the fraction of CME by disentangling the background through modified charged azimuthal correlators and provides an upper limit of 15-18% at 95% confidence level for mid-central collisions in Pb-Pb collisions [28]. The original three-particle charged azimuthal correlator is modified by correlating the charged particles with respect to the third order symmetry plane (Ψ_3) of the form $\gamma_{1,2} = \langle \cos(\varphi_\alpha + 2\varphi_\beta - 3\Psi_3) \rangle$, where Ψ_3 is very weakly correlated with $\Psi_2 \approx \Psi_{RP}$. The correlator $\gamma_{1,2}$ is expected to contain negligible CME signal (charge separation relative to the reaction plane), but it mainly reflects the background effects. In the background-only scenario, $\Delta\gamma_{1,1}$ and $\Delta\gamma_{1,2}$ can be approximated according to $\Delta\gamma_{1,1} \propto \kappa_2 \Delta\delta_1 v_2$ and $\Delta\gamma_{1,2} \propto \kappa_3 \Delta\delta_1 v_3$, where κ_2 and κ_3 are proportionality constants assumed to be approximately the same. This assumption is backed up by the study from the CMS collaboration at the LHC on charge-dependent azimuthal correlations in p-Pb and Pb-Pb collisions [38].

The spectator-plane-participant-plane method, proposed by [39, 40], was utilised in Au-Au collisions at $\sqrt{s_{NN}}$ = 200 GeV by the STAR collaboration [41]. In peripheral collisions, the analysis yields a signal consistent with zero. However, a hint of finite positive signal with a 1-3σ significance was concluded in mid-central Au-Au collisions. A final upper limit of the percentage of CME signal for full data within centrality interval 20-50% and $0.2 < p_T < 2$ GeV/c is given as 14.7 ± 4.3(stat.) ± 2.6(syst.)%.

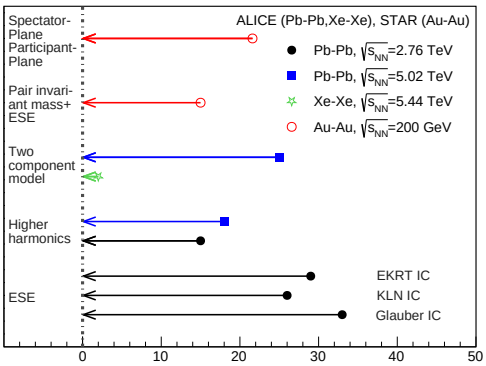

Figure 3: Summary of the results for the CME limit obtained from different analyses performed at various LHC and RHIC energies and colliding systems integrated over centralities. Data points are from [28, 30, 34, 37, 41].

More recently, the idea of using isobar collisions (two ions with same nucleon number but different proton number) was proposed to verify the CME [42]. The STAR Collaboration performed dedicated isobar collisions (Ru-Ru and Zr-Zr) and compared the CME sensitive observables among these two systems which are thought to have same level of background (same nucleon number in Ru and Zr) but different strength of CME owing to Ru and Zr having different proton number [43]. Although it was reported that no CME signature was observed, the background effects from Ru and Zr were realised later to be still different enough to overwhelm the small signal of CME. The LHC has not performed any isobar collisions, but inspired by the idea of isobar collisions, the ALICE collaboration studied the Xe-Xe

collisions at $\sqrt{s_{NN}}$ = 5.44 TeV and Pb-Pb collisions at $\sqrt{s_{NN}}$ = 5.02 TeV together using a two-component model [30]. The study resulted in an upper limit of around 2% and 25% at 95% confidence level for the 0–70% centrality interval in Xe–Xe and Pb–Pb collisions, respectively. The upper limits of CME from all ALICE studies at various collision energies and systems are summarized in Fig. 3. Overall, the current upper limits in Pb-Pb and Xe-Xe collisions suggest a higher potential to reveal CME in large collision systems (e.g. Pb–Pb) than in their small collision counterparts, mainly due to higher early magnetic field created by larger number of proton in large collision systems.

5 Conclusions

The early magnetic field created by spectator protons is of great experimental interest to be measured directly. The charge-dependent directed flow of oppositely charged particles as well as for D^0 and $\bar{D}^0$ measured by the ALICE and STAR collaboration provides the indication of the effect of the early electromagnetic fields on the motion of final state charged particles, especially to heavy-flavour hadrons. In addition, the CMS collaboration provides the limit of the charge-dependent elliptic flow of D^0 and $\bar{D}^0$ as $\Delta v_2 = 0.001 \pm 0.001(\text{stat.}) \pm 0.003(\text{syst.})$, showing no significant deviation from zero but a possible hint of its value opposite to the model prediction. An another independent approach to study the early magnetic field is to measure the global polarisation of Λ and $\bar{\Lambda}$, which gives an upper limit for the magnetic field at freeze-out of $eB/m_\pi^2 = 0.017$ (equivalent to 5.7×10^{12} T and 0.044 (or 14.4×10^{12} T) at a 95% confidence level in Pb-Pb collisions at $\sqrt{s_{NN}}$ = 2.76 and 5.02 TeV, respectively. The same measurements from RHIC in Au-Au collisions result in higher upper limits at lower collision energies from $\sqrt{s_{NN}}$ = 7.7 GeV to 200 GeV.

The extraction of the CME signal of the CME in heavy-ion collisions at the LHC and RHIC has been exceptionally challenging due to dominated background effects. Three methods, event shape engineering, higher harmonics and two-component model, based on charge dependent correlations relative to the reaction plane or the spectator plane have been attempted by the ALICE, and CMS collaboration and provide constrains on the CME signal to upper limits ranging from 7 to 33% (dependent on different studies) in Pb–Pb (ALICE and CMS) and 2% in Xe–Xe collisions (ALICE) at LHC energies at 95% confidence level. The combination of studies in Pb–Pb and Xe–Xe collisions suggests a higher potential to reveal CME in large collision systems (e.g. Pb–Pb) than in their small collision counterparts, mainly due to higher early magnetic field created by larger number of proton in large collision systems. In Au-Au collisions, upper of limits of 15 and 21.6% at 95% confidence level are provided by the STAR collaboration using event shape engineering+pair invariant mass and spectator-plane-participant-plane method, respectively. In addition, no significant deviation from background-only scenario is concluded by STAR from the isobar collisions at RHIC.

References

[1] V. Skokov, A.Y. Illarionov, V. Toneev, Int. J. Mod. Phys. A **24**, 5925 (2009), 0907.1396
[2] Y. Zhong, C.B. Yang, X. Cai, S.Q. Feng, Adv. High Energy Phys. **2014**, 193039 (2014), 1408.5694
[3] G. Inghirami, M. Mace, Y. Hirono, L. Del Zanna, D.E. Kharzeev, M. Bleicher, Eur. Phys. J. C **80**, 293 (2020), 1908.07605
[4] A. Dubla, U. Gürsoy, R. Snellings, Mod. Phys. Lett. A **35**, 2050324 (2020), 2009.09727
[5] U. Gürsoy, D. Kharzeev, K. Rajagopal, Phys. Rev. C **89**, 054905 (2014)

[6] U. Gürsoy, D. Kharzeev, E. Marcus, K. Rajagopal, C. Shen, Phys. Rev. C **98**, 055201 (2018), 1806.05288
[7] F. Becattini, I. Karpenko, M. Lisa, I. Upsal, S. Voloshin, Phys. Rev. C **95**, 054902 (2017), 1610.02506
[8] N.S. Manton, Phys. Rev. D **28**, 2019 (1983)
[9] F.R. Klinkhamer, N.S. Manton, Phys. Rev. D **30**, 2212 (1984)
[10] P. Arnold, L. McLerran, Phys. Rev. D **36**, 581 (1987)
[11] D.E. Kharzeev, L.D. McLerran, H.J. Warringa, Nucl. Phys. A **803**, 227 (2008), 0711.0950
[12] D. Kharzeev, R.D. Pisarski, M.H.G. Tytgat, Phys. Rev. Lett. **81**, 512 (1998), hep-ph/9804221
[13] D.E. Kharzeev, Annals Phys. **325**, 205 (2010), 0911.3715
[14] K. Fukushima, D.E. Kharzeev, H.J. Warringa, Phys. Rev. D **78**, 074033 (2008), 0808.3382
[15] S. Acharya et al. (ALICE), Phys. Rev. Lett. **125**, 022301 (2020), 1910.14406
[16] L. Adamczyk et al. (STAR), Phys. Rev. Lett. **112**, 162301 (2014), 1401.3043
[17] J. Adam et al. (STAR), Phys. Rev. Lett. **123**, 162301 (2019), 1905.02052
[18] S. Chatterjee, P. Bozek, Phys. Lett. B **798**, 134955 (2019), 1804.04893
[19] A.M. Sirunyan et al. (CMS), Phys. Lett. B **816**, 136253 (2021), 2009.12628
[20] S. Acharya et al. (ALICE), Phys. Rev. C **101**, 044611 (2020), 1909.01281
[21] L. Adamczyk et al. (STAR), Nature **548**, 62 (2017), 1701.06657
[22] S.A. Voloshin, EPJ Web Conf. **171**, 07002 (2018), 1710.08934
[23] (2022), 2211.04384
[24] S.A. Voloshin, Phys. Rev. C **70**, 057901 (2004)
[25] B.I. Abelev et al. (STAR), Phys. Rev. Lett. **103**, 251601 (2009), 0909.1739
[26] B.I. Abelev et al. (STAR), Phys. Rev. C **81**, 054908 (2010), 0909.1717
[27] K. Aamodt et al. (ALICE), Phys. Rev. Lett. **106**, 032301 (2011), 1012.1657
[28] S. Acharya et al. (ALICE), JHEP **09**, 160 (2020), 2005.14640
[29] V. Khachatryan et al. (CMS), Phys. Rev. Lett. **118**, 122301 (2017), 1610.00263
[30] (2022), 2210.15383
[31] S. Aziz (ALICE), Nucl. Phys. A **1005**, 121817 (2021), 2005.06177
[32] S. Schlichting, S. Pratt, Phys. Rev. C **83**, 014913 (2011), 1009.4283
[33] S. Pratt, S. Schlichting, S. Gavin, Phys. Rev. C **84**, 024909 (2011), 1011.6053
[34] S. Acharya et al. (ALICE), Phys. Lett. B **777**, 151 (2018), 1709.04723
[35] A.M. Sirunyan et al. (CMS), Phys. Rev. C **97**, 044912 (2018), 1708.01602
[36] J. Schukraft, A. Timmins, S.A. Voloshin, Phys. Lett. B **719**, 394 (2013), 1208.4563
[37] M.S. Abdallah et al. (STAR), Phys. Rev. C **106**, 034908 (2022), 2006.05035
[38] A.M. Sirunyan et al. (CMS), Phys. Rev. C **97**, 044912 (2018), 1708.01602
[39] H.j. Xu, J. Zhao, X. Wang, H. Li, Z.W. Lin, C. Shen, F. Wang, Chin. Phys. C **42**, 084103 (2018), 1710.07265
[40] S.A. Voloshin, Phys. Rev. C **98**, 054911 (2018), 1805.05300
[41] M.S. Abdallah et al. (STAR), Phys. Rev. Lett. **128**, 092301 (2022), 2106.09243
[42] W.T. Deng, X.G. Huang, G.L. Ma, G. Wang, Phys. Rev. C **94**, 041901 (2016), 1607.04697
[43] M. Abdallah et al. (STAR), Phys. Rev. C **105**, 014901 (2022), 2109.00131